Journal of Experimental Neuroscience

ORIGINAL RESEARCH

Organization of Estrogen-Associated Circuits in the Mouse Primary Auditory Cortex

Liisa A. Tremere, Kaiping Burrows‡, Jin-Kwon Jeong‡ and Raphael Pinaud

Departments of Physiology, Geriatric Medicine and ROCA, University of Oklahoma Health Sciences Center, Oklahoma City, OK, USA. Corresponding author email: raphael-pinaud@ouhsc.edu
‡These authors contributed equally to this work.

Abstract: Sex steroid hormones influence the perceptual processing of sensory signals in vertebrates. In particular, decades of research have shown that circulating levels of estrogen correlate with hearing function. The mechanisms and sites of action supporting this sensory-neuroendocrine modulation, however, remain unknown. Here we combined a molecular cloning strategy, fluorescence in-situ hybridization and unbiased quantification methods to show that estrogen-producing and -sensitive neurons heavily populate the adult mouse primary auditory cortex (AI). We also show that auditory experience in freely-behaving animals engages estrogen-producing and -sensitive neurons in AI. These estrogen-associated networks are greatly stable, and do not quantitatively change as a result of acute episodes of sensory experience. We further demonstrate the neurochemical identity of estrogen-producing and estrogen-sensitive neurons in AI and show that these cell populations are phenotypically distinct. Our findings provide the first direct demonstration that estrogen-associated circuits are highly prevalent and engaged by sensory experience in the mouse auditory cortex, and suggest that previous correlations between estrogen levels and hearing function may be related to brain-generated hormone production. Finally, our findings suggest that estrogenic modulation may be a central component of the operational framework of central auditory networks.

Keywords: 17β-estradiol, mammalian, estrogen receptor, auditory cortex

Journal of Experimental Neuroscience 2011:5 45–60

doi: 10.4137/JEN.S7744

This article is available from http://www.la-press.com.

Introduction

Historically, sex steroid hormones have been studied in the context of reproductive biology. It is now clear, however, that sex hormones influence nervous system function to shape an array of behaviors, from mood and pain sensitivity, to cognitive processes such as learning and memory.[1–3] The classic hormone 17β-estradiol (E2) has also been shown to influence the perceptual processing of sensory signals, with most studies centered in the auditory system. For instance, E2 levels during the menstrual cycle correlate with hearing thresholds and the fidelity of event-related potentials in humans.[4,5] Various hearing pathologies also occur in women suffering from Ullrich-Turner syndrome, who are deficient in E2.[6–8]

The link between auditory processing and E2 has also been documented in animal models. In mice, auditory recognition and phonotaxis are robustly shaped by E2 treatment and in mothers, but not virgins, suggesting that E2 oscillations around parturition shape the perceptual processing of acoustic signals.[9–11] Ovariectomization of monkeys and rodents significantly alters auditory brainstem responses (ABRs); interestingly, estrogen-replacement therapy recovers normal ABR profiles.[12,13] Finally, mice that are deficient in estrogen receptor-β display severe progressive hearing loss that leads to early deafness.[14]

Although the observations above suggest that circulating E2 may affect hearing function, recent findings obtained in songbirds have markedly changed our understanding of how steroid hormones shape auditory processing. Specifically, E2 was shown to be rapidly produced by auditory forebrain neurons, in an experience-dependent manner.[15] Our group recently demonstrated that this brain-generated E2 increases the gain of auditory-driven responses, in real-time, by suppressing inhibitory neurotransmission via a non-genomic, pre-synaptic mechanism.[16] Finally, we also showed that one of the functional consequences of E2 produced by central auditory neurons is to increase the information carried about stimulus structure to enhance the neural and behavioral discrimination of sounds.[17] These findings provided direct evidence, and a mechanistic basis, for E2's modulation of auditory processing and highlighted a sex hormone as a major component of the neural substrates supporting auditory-based behaviors.

Here we show that the mouse AI is heavily endowed with estrogen-related networks; thus, the presence of robust estrogen-associated circuits may be a general property of the vertebrate auditory forebrain. Specifically, we first cloned the mouse genes encoding the estrogen-synthetic enzyme aromatase (ARO), and each of the classic estrogen receptors (ERα and ERβ). We next carried out a detailed expression analysis by in-situ hybridization and found that estrogen-producing and estrogen-responsive neurons are highly abundant in AI. We further show that estrogen-producing and -responsive neurons are directly engaged by auditory experience, and that estrogen-associated circuits are highly stable in response to acute sensory input. Finally, we demonstrate the neurochemical identity of estrogen-associated networks in AI, and show that such circuits are functionally heterogeneous. Our findings provide the first demonstration that the mammalian AI is a site of a major sensory-neuroendocrine overlap, and emphasize that central auditory processing may be heavily modulated by brain-generated E2.

Material and Methods

Animals

We used a total of 24 CBA/CaJ mice (n = 12 males and 12 females). All animals used were young adults (16–22 weeks old) at the time of experimentation. The OUHSC's Institutional Animal Care and Use Committee approved all animal use protocols, which were also in accordance with NIH's guidelines. No sex or hemispheric differences were detected in any of the parameters analyzed in this work; therefore, data was combined for males and females, as well as across hemispheres. Analyses were conducted in the primary auditory cortex, and more specifically the primary auditory field (AI), as anatomically and functionally defined by Stiebler and colleagues.[18] Anatomical and cortical layer boundaries were established using standard cytoarchitectonic criteria based on Nissl histochemistry.[19,20]

Auditory stimulation and tissue preparation

Mice were individually placed overnight in sound proof boxes (~76 × 31 × 28 cm), under a 14 h light: 10 h dark regimen, with lights on at 6:00 am. The next

day, animals were either kept in silence (unstimulated controls; n = 6), or were stimulated for 30 min (n = 6), 1 h (n = 6) or 2 h (n = 6) with a pseudo-randomized series of pure-tones that ranged from 1 kHz to 50 kHz, in 250 Hz intervals (stimulus duration: 50 ms; inter-stimulus interval: 450 ms; 70 dB mean SPL). Each tone encompassed 5 ms-long raised cosine on and off ramps that were applied to the beginning and end of each tone, respectively. Importantly, the stimulus range used in our studies spans the full frequency representation of the mouse primary auditory field.[18] For simplicity, experimental groups will be referred to as controls, 30 min, 1 h and 2 h groups, respectively, in the remainder of the text. This stimulation protocol has been repeatedly shown to consistently and robustly induce the mRNA expression of the early growth response-1 gene (*egr-1*; a.k.a., *zif268*, *NGFI-A* and *krox-24*), an activity-dependent immediate early gene whose expression reliably reveals hearing-driven neurons in AI (for review, see [21]).

Animals in each group were rapidly decapitated. All brains were extracted, embedded in Tissue-Tek (Sakura Finetek, Torrance, CA) and rapidly frozen in a dry-ice/ethanol bath. For unbiased stereological analysis of single- and double-labeled neurons, we carried out systematic-uniform-random (SUR) sampling of brain sections collected through the AI (detailed below). To this end, brains were cut coronally on a cryostat, were mounted on Superfrost Plus slides (Fisher Scientific, Pittsburgh, PA) and kept in a –80 °C freezer until used.

Aromatase, ERα and ERβ cloning

Antibodies raised against estrogen receptors (ERs) are notoriously problematic as they relate to specificity issues.[22] To avoid these limitations, we opted to clone the mouse ARO, ERα and ERβ genes, and use these cDNAs to generate riboprobes for in-situ hybridization, an approach that is highly reliable, sensitive and widely used to probe the molecular organization of brain regions. Furthermore, recent protocols for fluorescence in-situ hybridization, both developed and used by our group, provide highly stringent mRNA detection at single-cell resolution.[16,23,24]

In order to clone ARO, ERα and ERβ, we first obtained sequences for each of these genes from GenBank, from multiple species, including the mouse sequences (GenBank accession numbers: D00659.1, NM007956.4 and NM010157.3, respectively). These sequences were aligned and primer pairs were designed to amplify, via polymerase chain reaction (PCR), fragments associated with each gene from a mouse brain cDNA library (Biomatik Corp., Wilmington, DE). The primer pairs used were (ARO—forward: 5′-ACTTAAAGCTTGATCCACACTGT TGTGGGTGACAGA-3′; reverse: 5′- ACTTAG-GATCCTTCCATGTAATTACGGATAAGTAAT-GCC-3′; ERα—forward: 5′-ACTTAAAGCTTTG GCCTTGCTGCACCAGATCCAAGG-3′; reverse: 5′- ACTTAGGATCCGCCAGAGGCATAGTCATT-GCACACGGCAC-3′; ERβ—forward: 5′-ACTTAA AGCTTGTGACAGATGCCCTGGTCTGGGTGA-3′; reverse: 5′- ACTTAGGATCCTCCAGAACTCT-TAAGATGTTTTCCAAGTG-3′.

Amplification consisted of 30 PCR cycles, each encompassing 95 °C for 45 s, 44 °C for 1 min and 62 °C for 45 s and including Taq polymerase and standard PCR buffer. Each of the fragments amplified was 560 bp long and spanned from exon 6 to the 3′-untranslated region (UTR), from exons 2 to 6, and from exon 5 to the 3′-UTR of the ARO, ERα and ERβ genes of the mouse, respectively (Fig. 1). The amplified fragment of each gene was cloned in pBluescript SK^+ and their identity was confirmed through sequencing.

Northern blot analysis

We extracted total RNA from the forebrain of an adult male mouse following the protocol detailed by Chomczynski and Sacchi.[25] A sample of 10 µg of RNA was run on a standard MOPS-formaldehyde gel and blotted onto a nylon filter, using standard methods and protocols.[26] ^{33}P-labeled antisense riboprobes for ARO, ERα and ERβ were separately hybridized to the nylon filters using protocols that we described previously.[27,28]

Fluorescence in-situ hybridization (FISH)

Synthesis of Riboprobes: We used the QIAprep Spin miniprep kit (QIAGEN Inc., Valencia, CA) to purify plasmids containing: 1) ARO, a marker for estrogen-producing neurons[29–31] 2) ERα[31,32] and 3) ERβ,[31,33,34] both of which are markers for

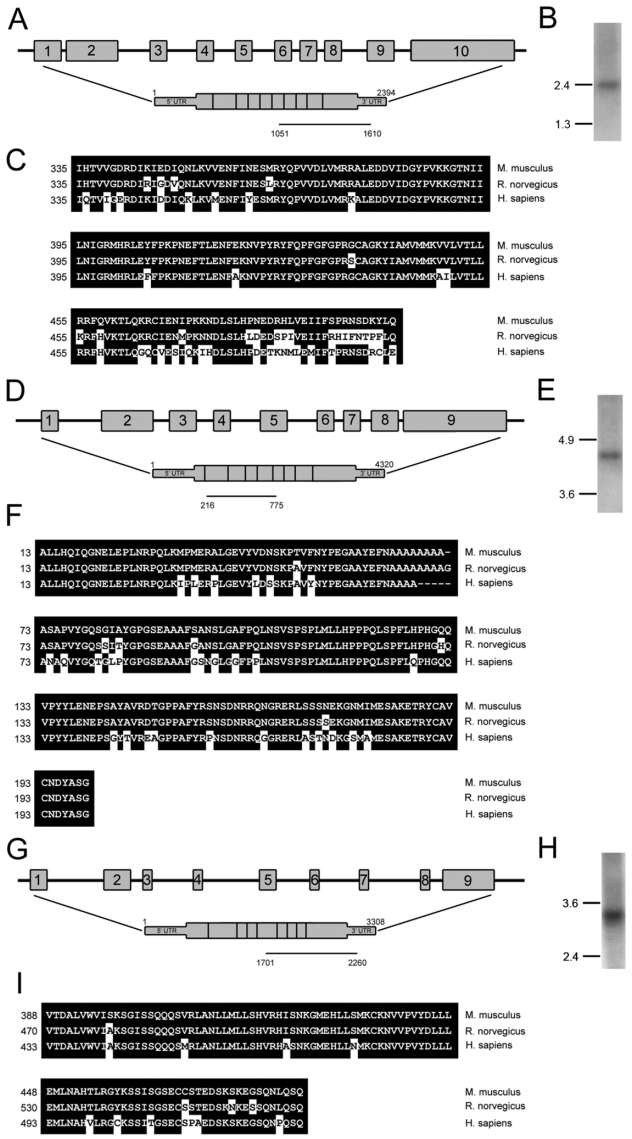

Figure 1. Cloning of ARO, ERα and ERβ. (**A**) Schematic representation of the mouse ARO gene. Whereas the boxes on the top schematic illustrate exons, the bottom schematic represents the cDNA structure. The solid line beneath the cDNA illustrates the location of the cloned fragment, along with the nucleotides spanned in the cDNA sequence (numbers). (**B**) Northern-blot of total forebrain RNA from an adult mouse probed with a ^{33}P-labeled ARO riboprobe. A single band is detected by the probe, of approximately 2.4 Kb in size. (**C**) Alignment of the predicted aminoacid sequences of the cloned ARO fragment against those of the rat and human homologues. Black boxes indicate residue identity. (**D**) Representation of the mouse ERα gene. While boxes on the top schematic highlight exons to scale, the bottom schematic represents the cDNA structure. The solid line underneath the cDNA depicts the location of the cloned fragment, along with the nucleotides spanned in the cDNA sequence (numbers). (**E**) Northern-blot probed with a ^{33}P-labeled ERα riboprobe. The riboprobe detected a single band of approximately 4.6 Kb in size. (**F**) Predicted aminoacid sequence alignment of the cloned ERα fragment against the homologue sequences in the rat and human. (**G**) Schematic representation of the mouse ERβ gene. Boxes on the top schematic depict exons and the bottom schematic represents the cDNA structure. The location of the cloned fragment is indicated by the solid line underneath the cDNA, along with the nucleotides spanned in the cDNA sequence (numbers). (**H**) Northern-blot probed with a ^{33}P-labeled ERβ riboprobe revealing a single band of approximately 3.4 Kb in size. (**I**) Alignment of the predicted aminoacid sequences of the cloned ERβ fragment and the rat and human homologues.

estrogen-sensitive cells; 4) *egr-1*, a marker for hearing-driven neurons;[21,35] 5) GAD65, a classic marker for GABAergic neurons[36,27] and 6) *vGlut2*, a standard marker for excitatory neurons.[37,38]

Plasmids were excised by exposure to the appropriate restriction enzymes and inserts were purified with QIAquick PCR Purification Kit (QIAGEN Inc., Valencia, CA). These inserts were used to generate both sense and antisense riboprobes via in-vitro transcription using protocols that we have described in detail previously.[16,23,24] Briefly, riboprobes were synthesized using a nucleotide labeling mix that contained digoxigenin (DIG)-tagged uridine triphosphate (UTP; Roche Diagnostics Corp.). Probes were purified in Sephadex G-50 columns. The protocols used to assemble our Sephadex columns have also been described previously.[23] A total of 1 ng/µl of purified riboprobe was used for each brain section. This volume was added to 16 µl of hybridization buffer (50% formamide, 2 × SSPE, 1 µg/µl BSA, 1 µg/µl poly A, 2 µg/µl tRNA in DEPC-treated water).

Hybridization Protocol: We have previously developed and described in detail our FISH protocols,[16,23,24] and therefore provide below only a condensed version of our method.

Sections were fixed in 3% paraformaldehyde in 0.1M PBS for 5 min, washed in 0.1M PBS and dehydrated in 70%, 95% and 100% ethanol. Tissue was then incubated in an acetylation solution (1.35% triethanolamine and 0.25% acetic anhydride in DEPC-treated water), rinsed in 2 × SSPE, dehydrated in the alcohol series described above, allowed to air-dry and then was incubated in the hybridization solution containing our probe(s) of interest, as described above. Sections were then coversliped, sealed by immersion in a mineral oil bath and incubated overnight at 65 °C. Following this hybridization step, excess oil was cleared by rinsing slides in chloroform. Slides were then decoversliped in 2 × SSPE, washed in 2 × SSPE (1 h at room temperature [RT]), 1.5 h in 2 × SSPE + 50% formamide and twice in 0.1 × SSPE (65 °C, 30 min each). Sections were subsequently incubated in 0.3% hydrogen peroxide in TNT buffer (0.1M Tris-HCl, pH = 7.4, 0.05% Triton-X 100 and 5M NaCl in DEPC-treated water; 3 × 10 min), in TNB buffer (TNT buffer + 2 mg/ml BSA for 30 min), and in a solution containing an HRP-coupled anti-DIG antibody (2 h at RT; 1:200 in TNB, Roche Diagnostics

Corp., Indianapolis, IN, USA). Subsequently, tissue was sequentially washed in TNB buffer (3 × 10 min), incubated for 30 min a solution containing tyramide-coupled Alexa 488 (1:200 in amplification buffer, provided by manufacturer; Invitrogen, Carlsbad, CA, USA), washed in TNT buffer (3 × 10 min), incubated in a solution containing the nuclear marker Hoechst (1:1000), washed in TNT buffer (3 × 10 min), and coversliped with Aquamount (Lerner Labs, Pittsburgh, PA, USA). Controls included hybridization of the sense strand, and incubations where the anti-DIG antibody was omitted; neither of which yielded detectable signal for any of the mRNAs analyzed.

Double fish (dFISH)

To label two mRNA species at single cell resolution, we used a dFISH protocol that we developed and previously described in detail.[23,24] In brief, antisense riboprobes of interest were co-hybridized in individual brain sections (e.g., *egr-1* and ARO, or GAD65 and ERβ). For each double-labeling combination, one riboprobe was labeled with DIG, as detailed above for single FISH, and the other riboprobe was labeled with biotin, using a nucleotide labeling mix containing biotin-tagged UTP (Roche Diagnostics Corp.). Sections were hybridized and washed, as described above for FISH, and then sequentially incubated in an HRP-conjugated anti-biotin antibody solution for 2 h at RT (1:300 in TNT buffer; Vector Laboratories, Burlingame, CA), and in a solution containing tyramide coupled with Alexa-594 for 45 min at RT (1:500 in TNT buffer). Peroxidase inactivation associated with the biotin-tagged riboprobe was carried out by incubating sections in 0.3% hydrogen peroxide for 10 min at RT. Next, the second riboprobe was detected via a sequential incubation of sections in solutions containing an HRP-conjugated anti-DIG antibody (2 h at RT; 1:100 in TNB buffer), tyramide coupled to Alexa-488 (45 min at RT; 1:200 in amplification buffer, provided by manufacturer), TNT buffer (3 × 5 min at RT), Hoechst (5 min at RT; 1:1000 in TNT buffer) and TNT buffer (3 × 10 min). Sections were then coversliped with Aquamount (Lerner Labs, Pittsburgh, PA, USA). Importantly, for all dFISH studies, we also used the reverse combination of tyramide reagents, which did not result in either qualitative or quantitative differences in our results. Furthermore, we controlled the effectiveness of the peroxidase inactivation between riboprobe detections by conducting additional dFISH reactions where we omitted the anti-DIG antibody, in which case signal was only observed in the adequate filter. A final control included the omission of the anti-biotin antibody to verify the specificity of the biotin labeling.[23,24]

Unbiased stereological quantification and statistics

The number of cells positive for each riboprobe were quantified using the optical fractionator method in a single reference space (AI). To this end, counting was carried out on an Olympus AX-70 equipped with a motorized stage, appropriate filters and integrated with Neurolucida software (Micro Bright Field). For each brain section we outlined the boundaries of AI in each section using a low power objective (4×). Cells that were positive for our riboprobes were then counted using a high power objective (63×) with a guard volume of 2 μm. This guard volume was included to avoid artifacts on the sliced surface of the brain sections. The total number of labeled cells per unit area were quantified by using the following sampling fractions: area sampling fraction (area of sampling frame divided by area of the x-y sampling step), thickness sampling fraction (height of disector divided by thickness of the section), and section sampling fraction (number of sections sampled divided by total number of sections). Cells were only counted if at least two-thirds of a cytoplasmic continuum was clearly detectable around the nucleus. In addition, to reach counting criteria, neurons needed to exhibit an unlabeled nucleus and clearly defined nucleolus, the latter of which was visualized with the Hoechst counterstaining.

The percentages of cells labeled for each riboprobe of interest were calculated relative to the total number of neurons per area, which was quantified based on Hoechst staining. When Hoechst-stained sections are visualized under the proper filter, neurons exhibit lightly, non-homogeneously stained nuclei and conspicuous nucleoli, whereas glial cells usually display strongly, homogeneously stained nuclei.[37] Even within clusters, neurons can be readily identified with this counterstaining. Importantly, our neuronal numerical densities obtained with Hoechst were not significantly different from those obtained with

Nissl-stained sections. To obtain group means, values obtained for each animal were averaged, and compared using a standard analysis of variance (ANOVA) and Tukey post-hoc tests, with significance criterion set at $P < 0.05$.

Imaging and photomicrography

Images were taken with either a Nikon TE2000-E or an Olympus AX-70 epifluorescence microscope coupled to a Nikon Photometrics Cool Snap ES digital camera, or a Leica SP2 MP confocal microscope. All microscopes were connected to desktop computers equipped with Metamorph software, which was used for image acquisition. Final image plates were generated with Adobe Photoshop software.

Results

Cloning of aromatase, ERα and ERβ

We cloned the genes encoding the mouse homologues of the estrogen-synthetic enzyme aromatase (ARO), and each of the estrogen receptors (ERα and ERβ). To this end, we aligned the sequences for each gene from mouse, rat and human, and identified conserved domains that are shared across species. PCR primers were designed and used to selectively amplify fragments of each gene from a mouse cDNA library. We isolated fragments of 560 bp that spanned from exon 6 to the 3′-untranslated region (UTR), from exons 2 to 6, and from exon 5 to the 3′-UTR of the mouse ARO, ERα and ERβ, respectively (Fig. 1). Analyses of the predicted amino acid sequence of our fragments revealed that they exhibit significant homology with the sequences of ARO, ERα and ERβ in other species. Specifically, our ARO fragment exhibited a homology of 99% (rat) and 99% (human) at the nucleotide level, and 100% (rat) and 100% (human) at the aminoacid level (Fig. 1A–C). The ERα fragment displayed a homology of 100% (rat) and 98% (human) at the nucleotide level, and 100% (rat) and 100% (human) at the aminoacid level (Fig. 1D–F). Finally, our ERβ fragment showed a homology of 100% (rat) and 53% (human) at the nucleotide level, and 100% (rat) and 100% (human) at the aminoacid level (Fig. 1G–I). These cloned fragments spanned aminoacid residues 335–501, 13–199 and 433–530 (nucleotides 1051–1610, 216–775 and 1701–2260) of the full-length human ARO, ERα and ERβ, respectively (Fig. 1A, D, G).

We next carried out northern blot analyses of total brain RNA that was hybridized with radioactively (^{33}P)-labeled antisense riboprobes generated with our ARO, ERα and ERβ fragments. For each riboprobe we identified single bands of 2.4, 4.6 and 3.4 Kb (Fig. 1B, E, H). The sizes of these bands are precisely within the expected molecular weights of the full-length mRNAs for ARO, ERα and ERβ based on the human, rat and mouse sequences. No bands were detected when membranes were hybridized with sense riboprobes (not shown). Together, these findings indicate that we successfully cloned cDNA fragments associated with ARO, ERα and ERβ and that our riboprobes reliably identify the mRNAs encoded by each of these genes.

Aromatase and estrogen receptors are expressed in AI neurons

We next determined the distribution of estrogen-producing and estrogen-responsive cells in the AI of adult mice, via fluorescence in-situ hybridization, using a protocol that we developed and described in detail previously[16,23,24] (Fig. 2). This approach allowed us to selectively identify cell populations that express ARO, ERα and ERβ in AI, with single cell resolution, thereby allowing a stringent quantitative assessment of these neuronal populations using unbiased stereological methods (Fig. 3).

The general expression of ARO- and ER-positive neurons obtained with our antisense riboprobes were in close accordance with known distributions of these markers in the mammalian brain, including the hypothalamus and hippocampus. A detailed documentation of the anatomical distribution of ARO- and ER-positive cells will be presented elsewhere. The present study focuses on the AI.

Remarkably, we found that estrogen-producing (ARO-positive) neurons are highly prevalent in AI. In particular, ARO-positive neurons were expressed across all cortical layers, with the exception of layer I (Fig. 2A–C). The distribution of cells positive for ARO was largely homogeneous across layers. Highest numbers of ARO-positive neurons were detectable in supragranular layers (II/III), followed by the infragranular (V/VI) and granular (IV) cell layers. More specifically, we found that each cubic millimeter (mm^3) of AI contained 31.2 ± 2.2 (mean ± S.E.), 30.3 ± 2.3 and 29.5 ± 2.2 × 10^3 neurons that were positive for

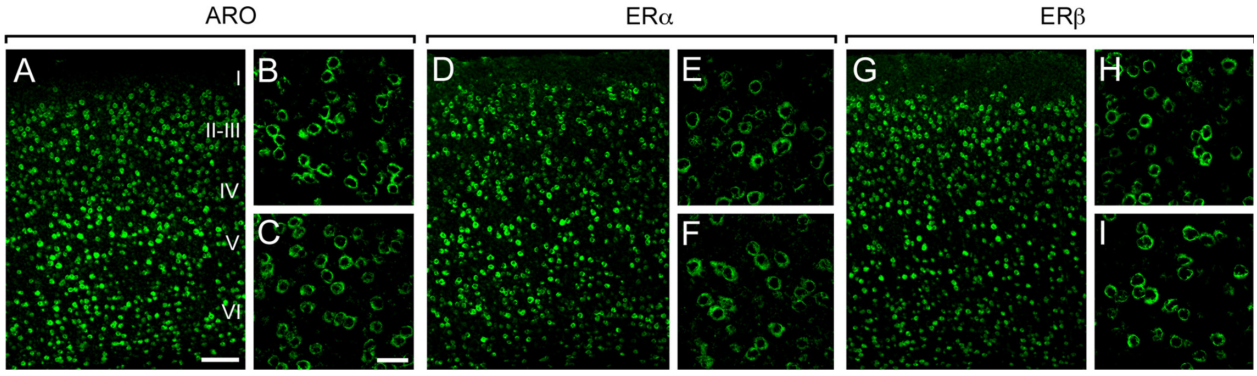

Figure 2. Estrogen-producing and estrogen-responsive neurons are highly prevalent and homogeneously distributed in the primary auditory cortex (AI). Fluorescence in-situ hybridization for ARO (A–C), ERα (D–F) and ERβ (G–I) in AI. For each gene, the long panels (A, D and G) depict low power photomicrographs of coronal sections obtained in AI highlighting the distribution of cells positive for each of the probed mRNAs. Note that ARO (A), ERα (D) and ERβ (G) are expressed at significant levels in AI, across all cortical layers, with the exception of layer I. The set of two smaller photomicrographs for each gene (B–C; ARO), (E–F; ERα) and (H–I; ERβ) depict representative high-power images obtained in supragranular (top) and infragranular (bottom) layers of AI showing detailed views of ARO-, ERα- and ERβ-positive cells in AI. Sense strand hybridization did not yield measurable signals for each of the genes studied (not shown). Low-power and high-power images were obtained with epifluorescence and confocal microscopy, respectively. Scale bars (in μm): 100 (A, D, G), 25 (B–C, E–F, H–I).

ARO in each of these layers, respectively (Fig. 3). Overall, when considering all cortical layers combined, ARO-positive neurons accounted for approximately 67% ± 3.9 of the overall neuronal population in AI.

The AI is also a site that is putatively sensitive to estrogens, as revealed by significant estrogen receptor expression (Fig. 2D–I). Although both estrogen receptors were expressed in AI neurons, ERα was found in a conspicuously smaller cell population than ERβ across cortical strata. Notably, with the exception of layer I, ERα-positive cells were homogeneously distributed within and across cortical layers

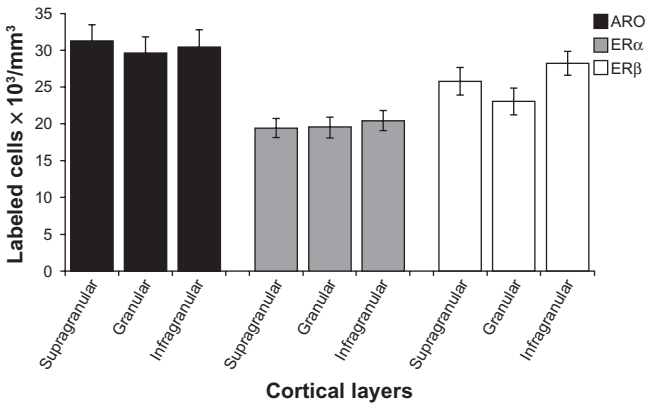

Figure 3. Estrogen-producing and estrogen-sensitive neurons constitute a significant fraction of the neuronal population of AI. Bar graphs depicting the mean (±S.E.) numerical densities of ARO-, ERα and ERβ-positive neurons, for supragranular (II/III), granular (IV) and infragranular layers (V/VI) of AI in adult mice. Measurements were obtained using unbiased stereology (see Methods).

of AI (Fig. 2D–F). Quantitative analyses revealed that AI contained 19.4 ± 1.3, 19.5 ± 1.4 and 20.4 ± 1.3 × 10^3 ERα-positive cells per mm^3, for supragranular, granular and infragranular layers, respectively (Fig. 3).

Neurons that were positive for ERβ were also expressed in cortical layers II/III, IV and V/VI, and their distribution was largely homogeneous within cortical layers (Fig. 2G–I). The density of ERβ-positive cells was more pronounced in the infragranular layers, followed by the supragranular and granular layers. Specifically, quantitative analyses revealed that AI contained 25.7 ± 1.8, 23.0 ± 1.7 and 28.1 ± 1.6 × 10^3 neurons that were positive for ERβ per mm^3, for supragranular, granular and infragranular layers, respectively (Fig. 3). When all cortical layers are considered together, we found that approximately 44% ± 2.2 and 57% ± 2.9 of the neuronal population of AI express ERα and ERβ mRNAs, respectively.

Finally, we investigated the degree of overlap between ARO and each of the ERs, to gain insight on whether locally-produced estrogen may be acting through paracrine and/or autocrine mechanisms. To this end, we used a double-FISH protocol that we developed and described in detail previously, to detect two mRNA species at single cell resolution (in this study ARO/ERα or ARO/ERβ).[23,24] Quantitative analyses revealed that whereas 21% ± 2.4 of ARO-positive cells co-expressed ERα mRNA, a total of 74% ± 2.6 of ARO-positive neurons were positive for the mRNA of ERβ. These results suggest that

locally-produced estrogen is well positioned to exert primarily paracrine effects on ERα-positive neurons, and autocrine and paracrine effects on cells that express ERβ.

Overall, the findings above indicate that the adult mouse AI is a site that contains a relatively high density of estrogen-producing and -responsive neurons. These results further suggest that estrogens, of peripheral and local (central) sources, may play a central role in the physiology of central auditory circuits.

Estrogen-associated networks are engaged by auditory stimulation

To directly test if estrogen-producing and -sensitive neurons are activated by auditory experience, we stimulated freely-behaving animals with a medley of pure-tones and used the expression of the activity-dependent immediate early gene *egr-1* (a.k.a., *NGFI-A*, *zif-268*, *krox-24* and *zenk*) to identify hearing-driven neurons (Fig. 4). This approach has been repeatedly and successfully used by multiple independent research groups to reliably identify neurons engaged by sensory experience in AI (reviewed in [21]). More specifically, we used our dFISH protocol to detect neurons that co-expressed *egr-1* and ARO, ERα or ERβ).[23,24]

We found that a significant population of ARO-positive neurons was engaged by auditory stimulation in AI, as revealed by *egr-1* mRNA co-localization (Fig. 4A–C). In particular, quantitative analyses revealed that 28.5 ± 1.8, 26.2 ± 1.9 and $28.1 \pm 1.8 \times 10^3$ cells/mm^3 were positive for both molecular markers in the supragranular, granular and infragranular layers of AI, respectively. When different cortical strata are considered together, our quantitative results indicated that approximately 83% ± 1.9 of AI's overall neuronal population engaged by auditory experience (as revealed by *egr-1* expression) are putatively estrogen-producing cells (as revealed by ARO expression). Importantly, these data also revealed that approximately 91% ± 2.0 of the ARO-positive neuronal population of AI is engaged by sensory input.

In stark contrast to the high numbers of ARO-positive cells activated by auditory stimulation, a significantly smaller fraction of estrogen-sensitive neurons (ER-positive) were engaged by sensory input relative to ARO population (Fig. 4D–I). More specifically, we found that 7.5 ± 0.7, 7.1 ± 0.6 and $8.5 \pm 0.6 \times 10^3$ cells/mm^3 in the supragranular,

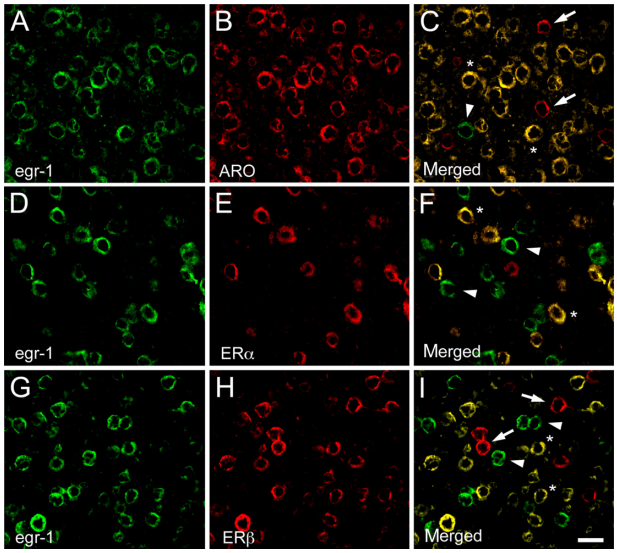

Figure 4. Estrogen-associated circuits are engaged by sensory experience. (A–C) Photomicrographs depicting double-fluorescence in-situ hybridization (dFISH) signal in the AI of mice stimulated with pure-tones, highlighting neurons that co-express the activity-dependent immediate early gene *egr-1* (A) and ARO (B) mRNAs. Representative neurons that are positive only for *egr-1* (arrowheads) or ARO (arrows), or double-labeled neurons (asterisks), can easily be distinguished in the merged image (C). (D–F) Representative dFISH signal depicting neurons that co-express *egr-1* (D) and ERα (E) mRNAs in AI. Cells that are positive only for *egr-1* (arrowheads) or ERα mRNAs (arrows) can be identified in the merged image (F), along with neurons that co-localize both mRNAs (asterisks). (G–I) Example of dFISH signal in AI depicting neurons that co-express *egr-1* (G) and ERβ (H) mRNAs in AI. Cells that are positive only for *egr-1* (arrowheads) or ERβ mRNAs (arrows) can be identified in the merged image (I) along with neurons that co-localize both mRNAs (asterisks). All images were obtained with confocal microscopy. Scale bar = 25 μm.

granular and infragranular layers of AI co-expressed the mRNAs for *egr-1* and ERα. Similarly, our stereological quantification revealed that 14.2 ± 1.2, 11.8 ± 1.1 and $14.8 \pm 1.1 \times 10^3$ neurons co-expressed *egr-1* and ERβ in supragranular, granular and infragranular layers, respectively. Together these findings show that approximately 23% ± 0.4 and 41% ± 0.7 of the overall population of hearing-driven neurons in AI, as revealed by *egr-1* expression, expresses ERα and ERβ, respectively. These data also revealed that nearly 39% ± 2.1 and 53% ± 2.0 of the population of ERα and ERβ-positive neurons are directly engaged by sensory experience. Notably, relative to the population of estrogen-producing neurons (ARO-positive), these findings suggest that a relatively small population of estrogen-sensitive neurons is activated by sensory experience.

Finally, in our preparations we reliably detected neurons that were labeled for a single riboprobe—i.e., hearing-activated (*egr-1*-positive) neurons that were

negative for ARO or each of the estrogen receptors (Fig. 4, arrowheads). This population putatively accounts for neurons activated by auditory experience that do not participate in estrogen-associated circuits. In addition, we routinely encountered cells that were part of estrogen-associated networks (ARO-, ERα or ERβ-positive), but that lacked hearing-driven *egr-1* mRNA expression (Fig. 4, arrows). This phenotype likely reflects neurons that were either not engaged by the acoustic features of our stimulus set, or that are not responsive to auditory stimuli. Consistent with previous reports, the number of *egr-1*-positive neurons in unstimulated controls was negligible.[21,39] Consequently, no quantification was carried out in this group.

In summary, the findings detailed above indicate that auditory experience in freely-behaving mice predominantly activates estrogen-producing neurons in AI, and to a lesser extent, estrogen-sensitive cells.

Estrogen-associated networks in AI are stable in response to acute sensory experience

We next probed the extent to which acute sensory experience affects the density of estrogen-producing and -sensitive neurons in AI. More specifically, we exposed different groups of animals to 30 min, 1 h or 2 h of auditory stimulation and quantified the density of ARO, ERα and ERβ-positive cells in AI, relative to unstimulated controls, which were kept in silence (see Methods) (Fig. 5). Quantification of our materials with unbiased stereological methods revealed that the density of ARO, ERα and ERβ-positive neurons for supragranular, granular and infragranular layers of AI were unaffected by auditory stimulation in all experimental groups, relative to control animals. In particular, we detected the following ARO-positive neuronal density per mm^3 of AI for control, 30 min, 1 h and 2 h groups, respectively. *Supragranular layers:* 30.1 ± 2.2, 29.5 ± 2.1, 31.8 ± 2.1 and 29.2 ± 2.3 × 10^3 ($F_{(3,20)} = 0.29$; $P = 0.83$). *Granular layer*: 28.3 ± 2.3, 29.7 ± 2.2, 30.1 ± 2.3 and 31.3 ± 2.2 × 10^3 ($F_{(3,20)} = 0.30$; $P = 0.82$). *Infragranular layers*: 31.1 ± 2.1, 29.2 ± 2.1, 29.8 ± 2.3 and 30.5 ± 2.3 × 10^3 neurons/mm^3 ($F_{(3,20)} = 0.13$; $P = 0.93$).

Similarly, acute auditory experience failed to significantly affect the number of ERα- and ERβ-positive neurons across cortical layers of AI (Fig. 5).

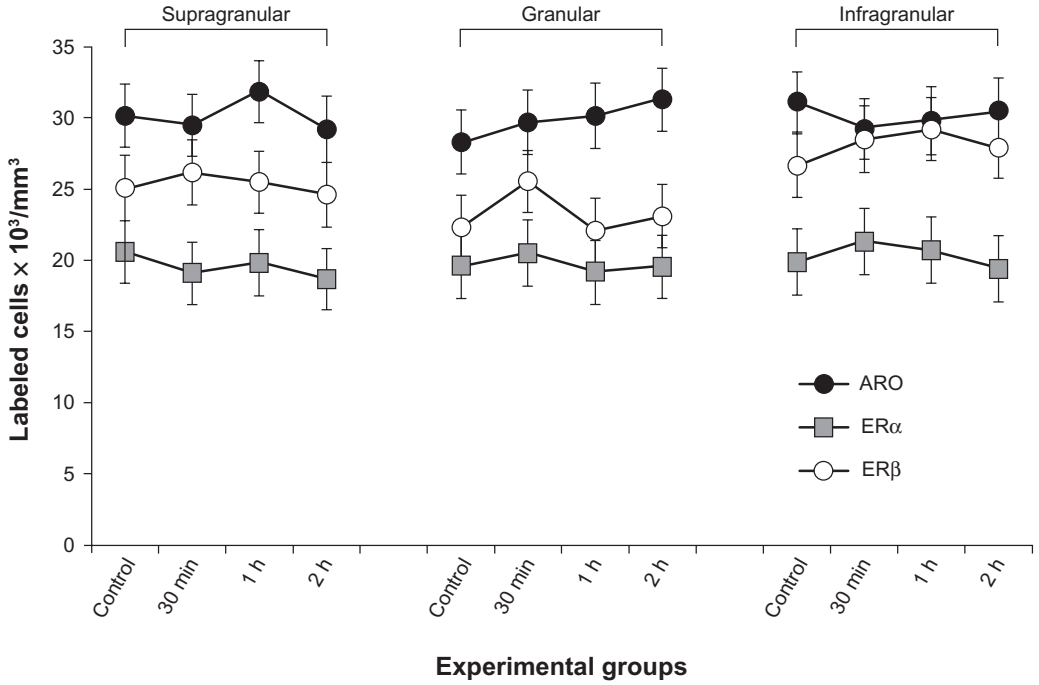

Figure 5. Acute sensory experience does not affect the density of ARO, ERα or ERβ-positive cells in AI. Shown are the mean (±S.E.) numerical densities of ARO-, ERα and ERβ-positive cells, for supragranular (II/III), granular (IV) and infragranular (V/VI) layers of the AI of adult mice that were maintained in acoustic isolation overnight (unstimulated controls), and that were exposed to 30 min, 1 h or 2 h of sensory stimulation (see Methods). Note that auditory experience failed to affect the density of ARO, ERα or ERβ-positive cells across cortical layers of AI.

More specifically, our quantitative analysis revealed the following number of ERα-positive neurons per mm^3 in the AI of control, 30 min, 1 h and 2 h groups, respectively. *Supragranular layers*: 20.6 ± 2.3, 19.1 ± 2.2, 19.8 ± 2.1, $18.7 \pm 2.2 \times 10^3$ ($F_{(3,20)} = 0.14$; $P = 0.93$). *Granular layer*: 19.6 ± 2.2, 20.5 ± 2.1, 19.2 ± 2.3, $19.5 \pm 2.2 \times 10^3$ ($F_{(3,20)} = 0.06$; $P = 0.98$). *Infragranular layers*: 19.9 ± 2.2, 21.3 ± 2.3, 20.7 ± 2.1 and $19.4 \pm 2.2 \times 10^3$ neurons/mm^3 ($F_{(3,20)} = 0.14$; $P = 0.93$). Likewise, no changes in the density of ERβ-positive neurons were detected as a result of acute sensory experience. For control, 30 min, 1 h and 2 h animals, respectively, we detected the following neuronal density per mm^3 of AI. *Supragranular layers*: 25.1 ± 2.2, 26.2 ± 2.1, 25.5 ± 2.3, $24.6 \pm 2.1 \times 10^3$ ($F_{(3,20)} = 0.09$; $P = 0.96$). *Granular layer*: 22.3 ± 2.3, 25.5 ± 2.2, 22.1 ± 2.2 and $23.1 \pm 2.1 \times 10^3$ ($F_{(3,20)} = 0.49$; $P = 0.68$). *Infragranular layers*: 26.6 ± 2.4, 28.5 ± 2.3, 29.2 ± 2.2 and $27.9 \pm 2.2 \times 10^3$ ($F_{(3,20)} = 0.23$; $P = 0.87$).

Overall, these findings suggest that both estrogen-producing and estrogen-responsive circuits in AI are stable in response to acute sensory experience. The possibility exists, however, that transcriptional activity of ARO, ERα and ERβ may be modulated by acute sensory experience. This question will be pursued in future studies.

Neurochemical identity of estrogen-associated networks in AI

To shed light into the neurochemical identity of estrogen-producing and -sensitive neurons in AI, we next conducted double-FISH studies combining riboprobes directed at ARO, ERα or ERβ, and classic markers for excitatory and inhibitory neurons, namely the vesicular glutamate transporter 2 (vGlut2) and the 65 kDa glutamic acid decarboxylase (GAD65), respectively (Fig. 6). Our stereological analyses revealed that 21.3 ± 1.8, 20.5 ± 1.7 and $19.8 \pm 1.7 \times 10^3$ neurons/mm^3 co-expressed ARO and vGlut2, and 8.0 ± 0.6, 9.4 ± 0.7 and $8.5 \pm 0.6 \times 10^3$ neurons/mm^3 were positive for both ARO and GAD65 in supragranular, granular and infragranular layers of AI, respectively (Fig. 6A–F). When considering all cortical layers combined, these results indicate that 67.6% ± 1.5 and 28.6% ± 0.6 of the population of ARO-positive cells in AI is composed of excitatory and inhibitory neurons, respectively (Fig. 7A).

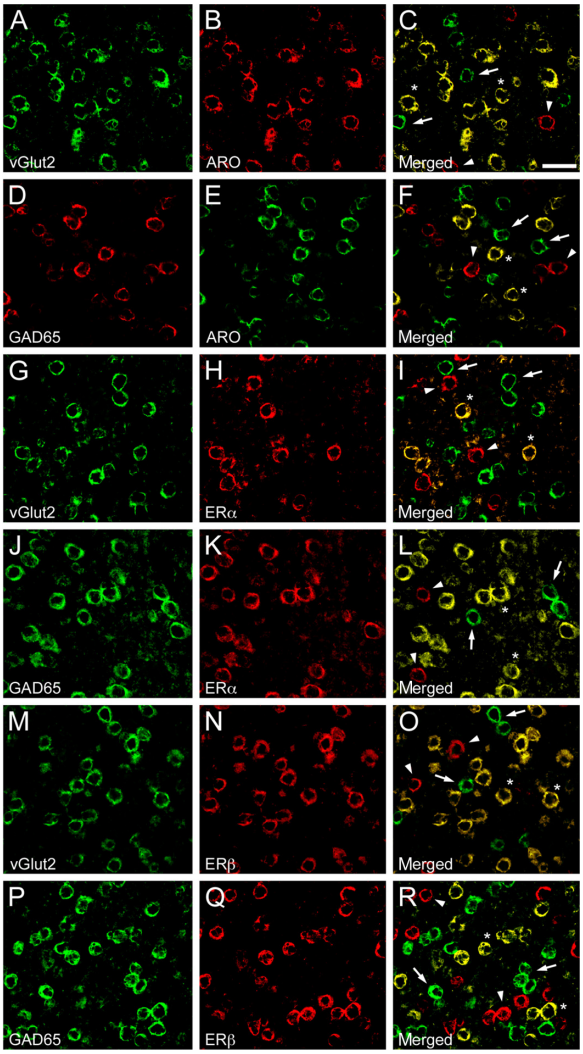

Figure 6. Estrogen-producing and -sensitive neurons in AI are neurochemically heterogenous. (A–F) Photomicrographs depicting dFISH signal for vGlut2, a marker for excitatory neurons (A) or GAD65, a marker for inhibitory neurons (D), and ARO (B, E) mRNAs in AI. Representative double-labeled neurons can be seen in the merged images (C, F) with asterisks, along with neurons that are positive only for ARO (arrowheads), or the neurochemical markers (arrows). (G–L) dFISH for vGlut2 (G) or GAD65 (J), and ERα mRNAs (H, K), reveals cells that are putatively sensitive to estrogen, and that exhibit either an excitatory or inhibitory phenotype. Examples of double-labeled neurons can be seen in the merged images (I, L), along with cells that are only positive for ERα (arrowheads), or labeled only for either vGlut2 or GAD65 mRNAs (arrows). (M–R) dFISH for vGlut2 (M) or GAD65 (P), and ERβ mRNAs (N, Q), reveals representative cells that are putatively sensitive to estrogen, and that exhibit either an excitatory or inhibitory phenotype. Examples of double-labeled neurons can be identified in the merged images (O, R), along with cells that are only positive for ERβ (arrowheads), or labeled only for either vGlut2 or GAD65 mRNAs (arrows). Images were obtained with confocal microscopy. Scale bar = 25 μm.

Interestingly, the populations of estrogen-sensitive neurons (ERα and ERβ) were neurochemically heterogeneous from each other. More specifically, we found that 2.3 ± 0.2, 2.7 ± 0.2 and $3.0 \pm 0.2 \times 10^3$ neurons/mm^3 were positive for both ERα and

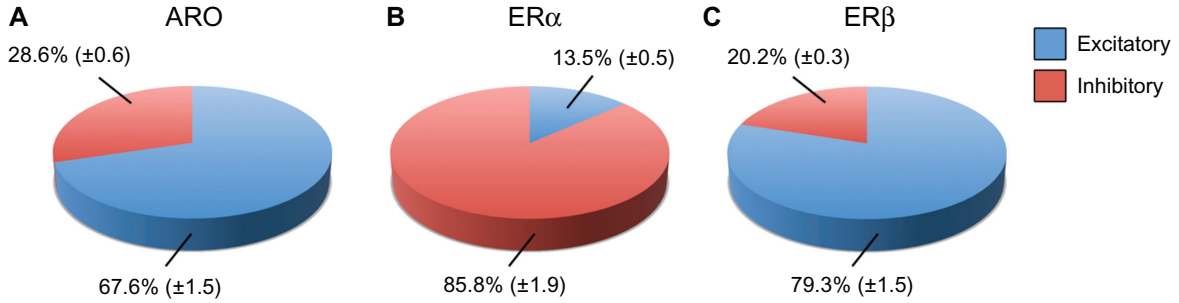

Figure 7. Neurochemical identity of estrogen-producing and -sensitive neurons in AI. Pie charts illustrate the percentage (±S.E.) of estrogen-producing (ARO-positive) and estrogen-sensitive (ERα and ERβ-positive) neurons that are putatively excitatory, as revealed by co-expression of vGlut2 mRNA, or inhibitory, as revealed by co-expression of GAD65 mRNA.

vGlut2, and 16.6 ± 1.7, 17.5 ± 1.4 and 17.1 ± 1.5 × 10^3 neurons/mm^3 were positive for ERα and GAD65 in supragranular, granular and infragranular layers of AI, respectively (Fig. 6 G–L). In contrast, quantification of neurons that were double-labeled for ERβ and vGlut2 mRNA revealed that the supragranular, granular and infragranular layers contained 20.6 ± 1.5, 18.8 ± 1.5 and 21.7 ± 1.6 × 10^3 neurons/mm^3, respectively. These cortical strata contained 5.4 ± 0.3, 3.9 ± 0.3 and 6.2 ± 0.4 × 10^3 neurons/mm^3 that co-expressed ERβ and GAD65 (Fig. 6M–R). These quantitative findings indicate that 13.5% ± 0.5 and 85.8% ± 1.9 of the population of ERα-expressing cells is composed of excitatory and inhibitory, respectively (Fig. 7B). In stark contrast, ERβ-positive neurons are primarily glutamatergic; specifically, we found that 79.3% ± 1.5 and 20.2% ± 0.3 of ERβ-positive cells are excitatory and inhibitory, respectively (Fig. 7C).

Overall, these data indicate that estrogen-associated circuits in AI are not uniform neurochemically, but rather encompass neuronal populations that are neurochemically biased towards predominantly excitatory (ARO and ERβ), or inhibitory (ERα) phenotypes.

Discussion

The results described above provided clear evidence that estrogen-associated circuits are highly prevalent in the mouse AI. In particular, using sensitive in-situ hybridization methods and unbiased quantitative approaches, we demonstrated that neurons expressing the estrogen synthetic enzyme ARO, and each of the estrogen receptors (ERα and ERβ) are heavily distributed throughout AI. We further demonstrated that estrogen-producing, and to a lesser extent estrogen-responsive, neurons are engaged by sensory experience. These cell populations are highly stable in response to acute auditory stimulation and remain quantitatively unchanged as a result of up to 2 h of sensory experience. Finally, we demonstrated that estrogen-producing and -sensitive neurons are neurochemically diverse. To our knowledge, this work provides the first demonstration of the robust presence of estrogen-associated circuits, their engagement by sensory experience, and their neurochemical identity, in the mammalian auditory cortex. Importantly, our findings are based on the detection of transcript levels. Future studies will be required to understand if and how such expression patterns may differ from protein levels.

Estrogen networks in the auditory cortex

Indirect links between E2 and auditory processing have been suggested in the literature for decades. For instance, fluctuations in auditory-event related potentials and hearing thresholds correlate positively with plasma E2 levels in humans throughout the menstrual cycle.[4,5] Women who suffer from Ullrich-Turner syndrome, and are deficient in E2, exhibit severe hearing pathologies, some of which can be recovered by estrogen-replacement therapy.[6–8] In fact, estrogen deficits caused by ovariectomies in rodents and monkeys drives marked distortions in ABRs, which can also be recovered by estrogen supplementation, suggesting a causal link between estrogenic regulation and hearing function.[12,13] These findings are congruent with recent observations that ERβ-deficient mice exhibit severe progressive hearing loss that leads to early deafness.[14] Together, these observations have

been overwhelmingly interpreted to suggest that gonadal E2 levels influence the functionality of the peripheral organ (cochlea). This interpretation is consistent with previous observations that estrogenic status in pregnant mice or mothers, differentially influence the auditory and perceptual processing of pup vocalizations relative to age-matched virgin mice.[9,10,40,41] Similar findings have been observed in other vertebrate species, suggesting that hormonal levels may directly shape the auditory processing of behaviorally-relevant sounds.[11,42–46] Importantly, recent findings obtained in songbirds have revealed the presence of both ARO and ERα in the inner ear.[47] Our results suggest that, in addition to the prevalent view that circulating E2 may affect hearing function, brain-generated E2, and more specifically E2 produced in AI, may locally and directly shape central auditory processing.

Our findings provide the first direct demonstration that a vast population of AI neurons is associated with local estrogen production and sensitivity—in the order of 70% and 50% of the overall neuronal population, respectively. These observations suggest that estrogenic modulation may play a central role in the physiology of auditory circuits in the mammalian brain. Although the present work focused on the expression of the classic intracellular estrogen receptors, the possibility exists that GPR30 may be expressed in the AI and, if so, could also modulate auditory processing. This prospect will be investigated in future studies.

Using activity-dependent gene expression in freely-behaving animals, we also showed that auditory experience primarily engages estrogen-producing, and to a lesser extent, estrogen-responsive neurons in AI. These findings support a model by which E2 levels in AI may be regulated by auditory experience, as opposed to a scenario where the sensitivity of AI neurons to sustained E2 levels may be modulated by sensory input. Consistent with this view, recent *in-vivo* microdialysis studies carried out in freely-behaving songbirds have shown that E2 levels are locally regulated by sensory experience in the auditory forebrain, in a timescale of minutes.[15] The present findings that estrogen-producing neurons are chiefly engaged by auditory experience suggest that a similar mechanism may be implemented in the mammalian AI; that is, local E2 levels may be rapidly controlled in an activity-dependent fashion in the auditory cortex. While future in-vivo microdialysis studies will be required to directly address this possibility, our current findings directly demonstrate that AI neurons are well positioned to be influenced by locally-produced E2, and suggest that this neurohormone may be a key modulator of central auditory processing.

Central auditory processing modulation by estradiol

We also found that both classic estrogen receptors are abundantly expressed in AI. Although ERα is expressed in a significant fraction of AI neurons, our quantitative analysis revealed that ERβ is the dominant receptor subtype in this cortical area. Importantly, we also showed that ERα and ERβ-expressing neurons are neurochemically distinct. Whereas the former is primarily expressed in GABAergic neurons, the latter is dominantly expressed in excitatory cells. Considering the disparate roles played by excitation versus inhibition in shaping AI receptive field tuning properties, our findings suggest that ERα- and ERβ-positive neurons may separately influence the processing of acoustic cues. For instance, whereas ERβ-positive cells may carry the brunt of incoming thalamo-cortical and intracortical excitatory drive, ERα-containing neurons may play a central role in functionally sharpening receptive fields towards narrower frequency tuning.[48–51] Importantly, in-vivo voltage-clamp recordings in the rodent AI have shown that excitatory and inhibitory inputs are temporally mismatched and that the length of inhibitory synaptic input is shorter than previously thought, supporting a more prominent role for inhibition in the construction of extra-classic receptive fields.[50–54] As such, the fact that ERα is almost exclusively expressed in GABAergic neurons suggest that E2's action on this receptor subtype may determine, or influence, several aspects of inhibitory receptive field properties, including lateral inhibition—a possibility that will be of key interest in future studies.

Despite decades of indirect suggestions that E2 may shape auditory processing, the notion that brain-generated E2 rapidly modulates central auditory processing in the awake brain was conclusively demonstrated in the songbird model in recent studies. More specifically, and consistent with the findings

presented here, it was recently shown that the songbird analogue of the mammalian auditory cortex produces E2 in an experience-dependent manner.[15] In addition, our research group showed that local blockade of estrogen receptors, or blockade of the local production of E2 in the songbird auditory cortex, robustly decreases hearing-evoked responses in awake animals, indicating that brain-generated E2 enhances the gain of central auditory neurons.[16] Notably, we also showed that this E2- dependent facilitation of auditory-evoked responses occurs in real-time (in a scale of seconds) through a mechanism that involves a presynaptic suppression of local GABAergic transmission.[16] Thus, in the songbird auditory forebrain, E2 enhances the gain of auditory responses by selectively decreasing inhibitory tone through the modulation of GABA release probability. Although future studies will be necessary to uncover if a similar mechanism is implemented in the rodent AI, our results suggest that ERα-positive cells, which are dominantly associated with inhibitory neurons, may regulate neuronal gain by shaping the strength of local GABAergic transmission. Although fast excitatory neurotransmission (non-NMDA) does not appear to modulate the physiology of auditory neurons in the songbird,[16] previous studies in the rodent hippocampus have demonstrated rapid non-genomic effects for E2 in regulating neuronal responses in this structure.[3,55,56] For instance, E2 increases the magnitude of AMPA, Kainate and NMDA receptor EPSCs and enhances long-term potentiation in the hippocampus.[3,55,57,58] These earlier studies indicate that, at least in the hippocampus, E2 robustly modulates glutamatergic transmission through non-genomic mechanisms. Importantly, our findings show that the vast majority of glutamatergic neurons in AI are associated with ERβ; thus, E2 may rapidly modulate excitatory transmission in auditory neurons through this receptor subtype. Such a possibility will be highly congruent with recent studies showing that excitatory neurotransmission is selectively and pre-synaptically regulated by ERβ in hippocampal neurons.[59] In summary, local production of E2, and the presence of neurochemically distinct neuronal populations expressing ERα and ERβ in AI, places this brain-generated hormone in a unique position to shape fundamental features of both excitatory and inhibitory receptive field tuning properties. Consequently, E2 produced by auditory cortical neurons may directly influence multiple aspects of central auditory processing.

Influence of estradiol on auditory-based behaviors

Using a combination of neurophysiological recordings coupled to local pharmacological manipulations in awake songbirds, and information theoretical methods, our group recently uncovered that one of the main functional consequences of E2's modulation of central auditory processing is to increase the information that central auditory neurons carry about stimulus structure, to enhance both the neural and behavioral discrimination of auditory signals.[17] In other words, we showed that auditory coding efficiency is enhanced by E2 produced by auditory neurons and, as a consequence, auditory discrimination in freely-behaving animals is optimized.[17] These findings are consistent with pharmacological studies indicating that behavioral preferences for auditory cues are markedly influenced by E2 produced by auditory neurons in songbirds.[60] Such observations are also congruent with multiple studies suggesting that estrogen status in mice directly influence the perceptual processing of behaviorally-relevant auditory cues (vocalizations) in mice.[9–11,42] Given the strong similarities between the organization of estrogen-associated circuits in the songbird auditory forebrain, and that of the mouse AI presented here, it is highly plausible that the recently uncovered functional roles for brain-generated E2 in auditory processing and discrimination are not special features of the avian brain, but rather reflect a general property of central auditory circuits in the vertebrate brain that went undetected and, consequently, unstudied. We suggest that an intimate sensory-neuroendocrine interaction at the level of the auditory cortex likely provides a neural substrate for the numerous correlative studies suggesting that E2 may influence hearing function. Our findings, however, emphasize the need to seriously consider that E2's modulation of auditory processing may occur in cortical areas, and via locally-generated hormone, as opposed to the prevalent view that functionality of the peripheral organ (cochlea) may be influenced by gonadal/circulating estrogen sources. While future studies will determine the extent to which peripheral- versus centrally-derived E2 may, independently or synergistically, modulate auditory

cortical function, the findings presented here raise three broad considerations. First, brain-generated E2 may be a key neuromodulator in central auditory circuits. As such, the study of rapid neurohormonal modulation may provide new insights on the operational rules of auditory circuits in the vertebrate brain. Second, the interaction between sensory circuits and estrogen-associated networks may provide a unique tool to probe how steroid hormones may influence neuronal physiology more globally—an issue that has been studied for decades in other contexts, such as hypothalamic control of reproductive behavior, or estrogenic modulation of hippocampal physiology. Third, and finally, as the link between E2 and auditory processing becomes progressively more studied in mammals, it will be important to establish if, and the extent to which, some aspects of hearing dysfunction co-occurs with hormonal deficits, as in the case of the well documented hearing loss that occurs in menopausal women, and in human and animal models of estrogen deficiency.[6,7,12–14] Up until now the co-occurrence of hormonal deficits and hearing dysfunction were not thought to be causally related and, consequently, were not thoroughly considered. However, the present findings raise the intriguing possibility that certain aspects of hearing loss may be (at least partially) caused by abnormal estrogen regulation or estrogen-insufficiency. Future studies should directly probe and shed significant light in these important issues.

Acknowledgments

This work was supported by grants from NIH/NIDCD (R01-DC-010181–01), NSF (1064684), the Schmitt Foundation, and an Endowment from the Reynolds Foundation (to R.P.). The authors declare no conflict of interests.

Disclosure

Author(s) have provided signed confirmations to the publisher of their compliance with all applicable legal and ethical obligations in respect to declaration of conflicts of interest, funding, authorship and contributorship, and compliance with ethical requirements in respect to treatment of human and animal test subjects. If this article contains identifiable human subject(s) author(s) were required to supply signed patient consent prior to publication. Author(s) have confirmed that the published article is unique and not under consideration nor published by any other publication and that they have consent to reproduce any copyrighted material. The peer reviewers declared no conflicts of interest.

References

1. McEwen B. Estrogen actions throughout the brain. *Recent Prog Horm Res*. 2002;57:357–84.
2. Craft RM, Mogil JS, Aloisi AM. Sex differences in pain and analgesia: the role of gonadal hormones. *Eur J Pain*. 2004;8:397–411.
3. Woolley CS. Acute effects of estrogen on neuronal physiology. *Annu Rev Pharmacol Toxicol*. 2007;47:657–80.
4. Davis MJ, Ahroon WA. Fluctuations in susceptibility to noise-induced temporary threshold shift as influenced by the menstrual cycle. *J Aud Res*. 1982;22:173–87.
5. Walpurger V, Pietrowsky R, Kirschbaum C, Wolf OT. Effects of the menstrual cycle on auditory event-related potentials. *Horm Behav*. 2004;46:600–6.
6. Hultcrantz M, Sylven L, Borg E. Ear and hearing problems in 44 middle-aged women with Turner's syndrome. *Hear Res*. 1994;76:127–32.
7. Hultcrantz M, Sylven L. Turner's syndrome and hearing disorders in women aged 16–34. *Hear Res*. 1997;103:69–74.
8. Gungor N, Boke B, Belgin E, Tuncbilek E. High frequency hearing loss in Ullrich-Turner syndrome. *Eur J Pediatr*. 2000;159:740–4.
9. Ehret G, Koch M, Haack B, Markl H. Sex and parental experience determine the onset of an instinctive behavior in mice. *Naturwissenschaften*. 1987;74:47.
10. Koch M, Ehret G. Estradiol and parental experience, but not prolactin are necessary for ultrasound recognition and pup-retrieving in the mouse. *Physiol Behav*. 1989;45:771–6.
11. Miranda JA, Liu RC. Dissecting natural sensory plasticity: hormones and experience in a maternal context. *Hear Res*. 2009;252:21–8.
12. Coleman JR, Campbell D, Cooper WA, Welsh MG, Moyer J. Auditory brainstem responses after ovariectomy and estrogen replacement in rat. *Hear Res*. 1994;80:209–15.
13. Golub MS, Germann SL, Hogrefe CE. Endocrine disruption and cognitive function in adolescent female rhesus monkeys. *Neurotoxicol Teratol*. 2004;26:799–809.
14. Simonoska R, Stenberg AE, Duan M, et al. Inner ear pathology and loss of hearing in estrogen receptor-beta deficient mice. *J Endocrinol*. 2009;201:397–406.
15. Remage-Healey L, Maidment NT, Schlinger BA. Forebrain steroid levels fluctuate rapidly during social interactions. *Nat Neurosci*. 2008;11:1327–34.
16. Tremere LA, Jeong JK, Pinaud R. Estradiol shapes auditory processing in the adult brain by regulating inhibitory transmission and plasticity-associated gene expression. *J Neurosci*. 2009;29:5949–63.
17. Tremere LA, Pinaud R. Brain-generated estradiol drives long-term optimization of auditory coding to enhance the discrimination of communication signals. *J Neurosci*. 2011;31:3271–89.
18. Stiebler I, Neulist R, Fichtel I, Ehret G. The auditory cortex of the house mouse: left-right differences, tonotopic organization and quantitative analysis of frequency representation. *J Comp Physiol A*. 1997;181:559–71.
19. Pinaud R, Vargas CD, Ribeiro S, et al. Light-induced Egr-1 expression in the striate cortex of the opossum. *Brain Res Bull*. 2003;61:139–46.
20. Basta D, Tzschentke B, Ernst A. Noise-induced cell death in the mouse medial geniculate body and primary auditory cortex. *Neurosci Lett*. 2005;381:199–204.
21. Mello CV, Pinaud R. Immediate early gene regulation in the auditory system. In: Pinaud R, Tremere LA, eds. *Immediate early genes in sensory processing, cognitive performance and neurological disorders.* New York: Springer-Verlag. 2006:35–56.
22. Snyder MA, Smejkalova T, Forlano PM, Woolley CS. Multiple ERbeta antisera label in ERbeta knockout and null mouse tissues. *J Neurosci Methods*. 2010;188:226–34.

23. Pinaud R, Mello CV, Velho TA, Wynne RD, Tremere LA. Detection of two mRNA species at single-cell resolution by double-fluorescence in situ hybridization. *Nat Protoc*. 2008;3:1370–9.
24. Pinaud R, Jeong JK. Duplex in situ hybridization in the study of gene co-regulation in the vertebrate brain. *Methods Mol Biol*. 2010;611:115–29.
25. Chomczynski P, Sacchi N. Single-step method of RNA isolation by acid guanidinium thiocyanate-phenol-chloroform extraction. *Anal Biochem*. 1987;162:156–9.
26. Sambrook J, Fritsch EF, Maniatis T. Molecular cloning: a laboratory manual, 2nd Edition. Cold Spring Harbor, NY: Cold Spring Harbor Laboratory. 1989.
27. Pinaud R, Velho TA, Jeong JK, et al. GABAergic neurons participate in the brain's response to birdsong auditory stimulation. *Eur J Neurosci*. 2004;20:1318–30.
28. Velho TA, Pinaud R, Rodrigues PV, Mello CV. Co-induction of activity-dependent genes in songbirds. *Eur J Neurosci*. 2005;22:1667–78.
29. Shen P, Campagnoni CW, Kampf K, Schlinger BA, Arnold AP, Campagnoni AT. Isolation and characterization of a zebra finch aromatase cDNA: in situ hybridization reveals high aromatase expression in brain. *Brain Res Mol Brain Res*. 1994;24:227–37.
30. Stromstedt M, Waterman MR. Messenger RNAs encoding steroidogenic enzymes are expressed in rodent brain. *Brain Res Mol Brain Res*. 1995;34:75–88.
31. Iivonen S, Heikkinen T, Puolivali J, et al. Effects of estradiol on spatial learning, hippocampal cytochrome P450 19, and estrogen alpha and beta mRNA levels in ovariectomized female mice. *Neuroscience*. 2006;137:1143–52.
32. Kia HK, Yen G, Krebs CJ, Pfaff DW. Colocalization of estrogen receptor alpha and NMDA-2D mRNAs in amygdaloid and hypothalamic nuclei of the mouse brain. *Brain Res Mol Brain Res*. 2002;104:47–54.
33. Shughrue P, Scrimo P, Lane M, Askew R, Merchenthaler I. The distribution of estrogen receptor-beta mRNA in forebrain regions of the estrogen receptor-alpha knockout mouse. *Endocrinology*. 1997;138:5649–52.
34. Gundlah C, Kohama SG, Mirkes SJ, Garyfallou VT, Urbanski HF, Bethea CL. Distribution of estrogen receptor beta (ERbeta) mRNA in hypothalamus, midbrain and temporal lobe of spayed macaque: continued expression with hormone replacement. *Brain Res Mol Brain Res*. 2000;76:191–204.
35. Herdegen T, Leah JD. Inducible and constitutive transcription factors in the mammalian nervous system: control of gene expression by Jun, Fos and Krox, and CREB/ATF proteins. *Brain Res Brain Res Rev*. 1998;28:370–490.
36. Erlander MG, Tillakaratne NJ, Feldblum S, Patel N, Tobin AJ. Two genes encode distinct glutamate decarboxylases. *Neuron*. 1991;7:91–100.
37. Fremeau RT, Jr., Troyer MD, Pahner I, et al. The expression of vesicular glutamate transporters defines two classes of excitatory synapse. *Neuron*. 2001;31:247–60.
38. Herzog E, Bellenchi GC, Gras C, et al. The existence of a second vesicular glutamate transporter specifies subpopulations of glutamatergic neurons. *J Neurosci*. 2001;21:RC181.
39. Pinaud R, Tremere LA, Penner MR, Hess FF, Robertson HA, Currie RW. Complexity of sensory environment drives the expression of candidate-plasticity gene, nerve growth factor induced-A. *Neuroscience*. 2002;112:573–82.
40. Haack B, Markl H, Ehret G. Sound communication between parents and offspring. In: Willott JF, ed. *The auditory psychobiology of the mouse.* Springfield, IL: Charles C Thomas Pub Ltd.; 1983:55–97.
41. Ehret G. Infant rodent ultrasounds—a gate to the understanding of sound communication. *Behav Genet*. 2005;35:19–29.
42. Lucas JR, Freeberg TM, Krishnan A, Long GR. A comparative study of avian auditory brainstem responses: correlations with phylogeny and vocal complexity, and seasonal effects. *J Comp Physiol A Neuroethol Sens Neural Behav Physiol*. 2002;188:981–92.
43. Sisneros JA, Bass AH. Seasonal plasticity of peripheral auditory frequency sensitivity. *J Neurosci*. 2003;23:1049–58.
44. Goense JB, Feng AS. Seasonal changes in frequency tuning and temporal processing in single neurons in the frog auditory midbrain. *J Neurobiol*. 2005;65:22–36.
45. Miranda JA, Wilczynski W. Female reproductive state influences the auditory midbrain response. *J Comp Physiol A Neuroethol Sens Neural Behav Physiol*. 2009;195:341–9.
46. Maney D, Pinaud R. Estradiol-dependent modulation of auditory processing and selectivity in songbirds. Front Neuroendocrinol:(in press)—D.O.I. 10.1016/j.yfrne.2010.1012.1002.
47. Noirot IC, Adler HJ, Cornil CA, et al. Presence of aromatase and estrogen receptor alpha in the inner ear of zebra finches. *Hear Res*. 2009;252:49–55.
48. Suga N, Zhang Y, Yan J. Sharpening of frequency tuning by inhibition in the thalamic auditory nucleus of the mustached bat. *J Neurophysiol*. 1997;77:2098–114.
49. Chen QC, Jen PH. Bicuculline application affects discharge patterns, rate-intensity functions, and frequency tuning characteristics of bat auditory cortical neurons. *Hear Res*. 2000;150:161–74.
50. Wehr M, Zador AM. Balanced inhibition underlies tuning and sharpens spike timing in auditory cortex. *Nature*. 2003;426:442–6.
51. Dorrn AL, Yuan K, Barker AJ, Schreiner CE, Froemke RC. Developmental sensory experience balances cortical excitation and inhibition. *Nature*. 2010;465:932–6.
52. Zhang LI, Tan AY, Schreiner CE, Merzenich MM. Topography and synaptic shaping of direction selectivity in primary auditory cortex. *Nature*. 2003;424:201–5.
53. Tan AY, Zhang LI, Merzenich MM, Schreiner CE. Tone-evoked excitatory and inhibitory synaptic conductances of primary auditory cortex neurons. *J Neurophysiol*. 2004;92:630–43.
54. Wehr M, Zador AM. Synaptic mechanisms of forward suppression in rat auditory cortex. *Neuron*. 2005;47:437–45.
55. Gu Q, Moss RL. 17 beta-Estradiol potentiates kainate-induced currents via activation of the cAMP cascade. *J Neurosci*. 1996;16:3620–9.
56. Foy MR. 17beta-estradiol: effect on CA1 hippocampal synaptic plasticity. *Neurobiol Learn Mem*. 2001;76:239–52.
57. Wong M, Moss RL. Long-term and short-term electrophysiological effects of estrogen on the synaptic properties of hippocampal CA1 neurons. *J Neurosci*. 1992;12:3217–25.
58. Bi R, Broutman G, Foy MR, Thompson RF, Baudry M. The tyrosine kinase and mitogen-activated protein kinase pathways mediate multiple effects of estrogen in hippocampus. *Proc Natl Acad Sci USA*. 2000;97:3602–7.
59. Smejkalova T, Woolley CS. Estradiol acutely potentiates hippocampal excitatory synaptic transmission through a presynaptic mechanism. *J Neurosci*. 2010;30:16137–48.
60. Remage-Healey L, Coleman MJ, Oyama RK, Schlinger BA. Brain estrogens rapidly strengthen auditory encoding and guide song preference in a songbird. *Proc Natl Acad Sci USA*. 2010;107:3852–7.